

## Moored Salinity Time Series Measurements at 0°, 140°W\*

MICHAEL J. MCPHADEN, H. PAUL FREITAG AND ANDREW J. SHEPHERD

*Pacific Marine Environmental Laboratory, National Oceanic and Atmospheric Administration, Seattle, Washington*

(Manuscript received 10 August 1989, in final form 7 February 1990)

### ABSTRACT

This study describes moored salinity time series measurements in a biologically productive equatorial upwelling regime in the Pacific Ocean (0°, 140°W). Data were collected at 26 m and at 100 m for 13 months during 1987–1988 using four SEACAT conductivity and temperature recorders equipped with optional antifouling attachments. Laboratory pre- and post-deployment calibrations indicate that the instrumental drift in SEACAT salinity measurements was typically <0.015 psu with a maximum of 0.055 psu for sequential 6–7 month long mooring deployments. Root mean square (rms) differences with CTD casts taken within a few nautical miles of the moorings were ~0.05 psu. These values are an order of magnitude smaller than the observed range of salinity variations. Little biogenic material was found on the SEACAT sensors on recovery. Thus, we infer that the antifouling attachments used were effective and that similar favorable results using SEACATs can be expected at other times and places in equatorial upwelling regimes.

### 1. Introduction

Salinity data are valuable in equatorial oceanographic studies for estimating the density stratification of the water column, for circulation tracer studies, as an indicator of fluctuations in precipitation minus evaporation, and for accurately estimating dynamic height variations (e.g., Emery and Dewar 1982; Wyrski and Kilonsky 1984; Kessler and Taft 1987; Lukas and Lindstrom 1987). The role of salinity in the dynamics of the equatorial oceans has also been recently discussed in the context of numerical model simulations (e.g., Cooper 1988). However, at present the time scales of salinity fluctuations in the equatorial ocean are poorly documented because most data have been collected from relatively infrequent shipboard surveys. Time series of surface and upper ocean salinity with approximately monthly resolution exist in a few regions based on data from ships-of-opportunity (e.g., Donguy and Dessier 1984) and research cruises (e.g., Wyrski and Kilonsky 1984) but it is not known how these and more coarsely resolved time series may be aliased by shorter time scale fluctuations.

We have, therefore, begun to study the feasibility of making systematic multiyear moored time series mea-

surements of salinity as part of the Tropical Ocean Global Atmosphere (TOGA) program (National Academy of Science, 1988). Deployments of several months duration at a time are anticipated, so it is important that the sensors be resistant to biofouling in the highly productive equatorial upwelling regime; and that the sensor circuitry be stable to long-term drift. The only previous moored salinity time series in the equatorial oceans was a 4-month record collected during the Tropic Heat Experiment (Eriksen 1985) near 0°45'S, 140°W using an inductive salinometer mounted on a profiling current meter (Personal communication, Eriksen 1989). The expected accuracy of these measurements was about 0.01 psu based on an earlier three month deployment in the Sargasso Sea (Eriksen 1987). Inductive salinometers are not well-suited for our purposes though, since self-contained, high precision, commercially produced instruments are not readily available at relatively low cost. In contrast, since 1986 SeaBird Electronics, Inc. has marketed the SEACAT, a self-contained, lightweight (4.6 kg), relatively inexpensive electromechanical conductivity cell that would be appropriate for our applications provided that biofouling did not seriously degrade the accuracy of the measurements. Growth of organisms can significantly change the sensitivity of electromechanical conductivity cells, causing a possible spurious drift towards lower calculated salinities. Brown et al. (1987) for example reported instrumental drifts of 0 (1) psu per month during springtime blooms in the North Atlantic using an earlier version of the SEACAT sensors. Hence, we felt it necessary to examine the stability and accuracy of the SEACAT in a set of field experiments

\* Contribution No. 1143 from NOAA/Pacific Marine Environmental Laboratory.

Corresponding author address: Dr. Michael J. McPhaden, NOAA, Environmental Research Laboratories, Pacific Marine Environmental Laboratory, NOAA Building Number 3, 7800 Sand Point Way N.E., Seattle, WA 98115.

consisting of 6–7 month long deployments in an equatorial upwelling regime. This note reports on the results of these experiments.

## 2. Instruments and methods

The Seabird Model SBE-16 SEACAT (Fig. 1) measures temperature from an externally mounted, pressure protected, shock- and vibration-resistant, aged thermistor. Conductivity is measured from three platinized electrodes embedded in a glass conductivity cell. Electrodes were exposed to the environment so we obtained an optional antifouling device consisting of porous cylindrical conductivity cell attachments impregnated with tributyltin oxide. The manufacturer indicates that this compound should protect against fouling for six months to one year, depending on biological activity and flow rate past the sensors.

For each measurement, a resistance is converted to a frequency using high-precision patented Wein Bridge circuitry (Pederson and Gregg 1979). Frequencies are stored internally in solid state memory as 16-bit words. Data are extracted via an RS-232 interface, converted to temperature and conductivity using manufacturer-supplied calibration equations and combined to yield salinity via standard algorithms (Fofonoff et al. 1983).

Table 1 summarizes SEACAT manufacturer specifications. The temperature and conductivity sensor

TABLE 1. Manufacturer's specifications for the Model SBE-16 SEACAT.

	Temperature	Conductivity
Range	$-5^{\circ}\text{C}$ to $35^{\circ}\text{C}$	0 to $7\text{ S m}^{-1}$
Resolution	$0.001^{\circ}\text{C}$	$0.0001\text{ S m}^{-1}$
Accuracy	$0.01^{\circ}\text{C}$ (6 months) $^{-1}$	$0.001\text{ S m}^{-1}$ month $^{-1}$
Sensor response time	Variable $(72\text{ m s}^{-1} @ 1\text{ m s}^{-1}$ water velocity)	Variable O ( $100\text{ m s}^{-1}$ )

resolutions are given as  $0.001^{\circ}\text{C}$  and  $0.0001\text{ S m}^{-1}$ , respectively. Accuracy for temperature and conductivity is stated in terms of drift stability:  $0.01^{\circ}\text{C}$  (6 months) $^{-1}$  and  $0.001\text{ S m}^{-1}$  month $^{-1}$ , respectively. Note that  $0.1\text{ S m}^{-1}$  in conductivity translates roughly into 1 psu in salinity.

We deployed 4 SEACATs over a 13-month period from October 1987–November 1988 on taut-wire current meter moorings at  $0^{\circ}$ ,  $140^{\circ}\text{W}$ . Two consecutive deployments were made lasting about 7 and 6 months, respectively. The moorings were equipped with a surface-following toroidal buoy and were anchored in water depths of 4330–4350 m. SEACATs were mounted on the mooring line at 26 m and 100 m and oriented so as to provide flushing of the conductivity cell by the horizontal flow field (Fig. 1a). Once deployed though,

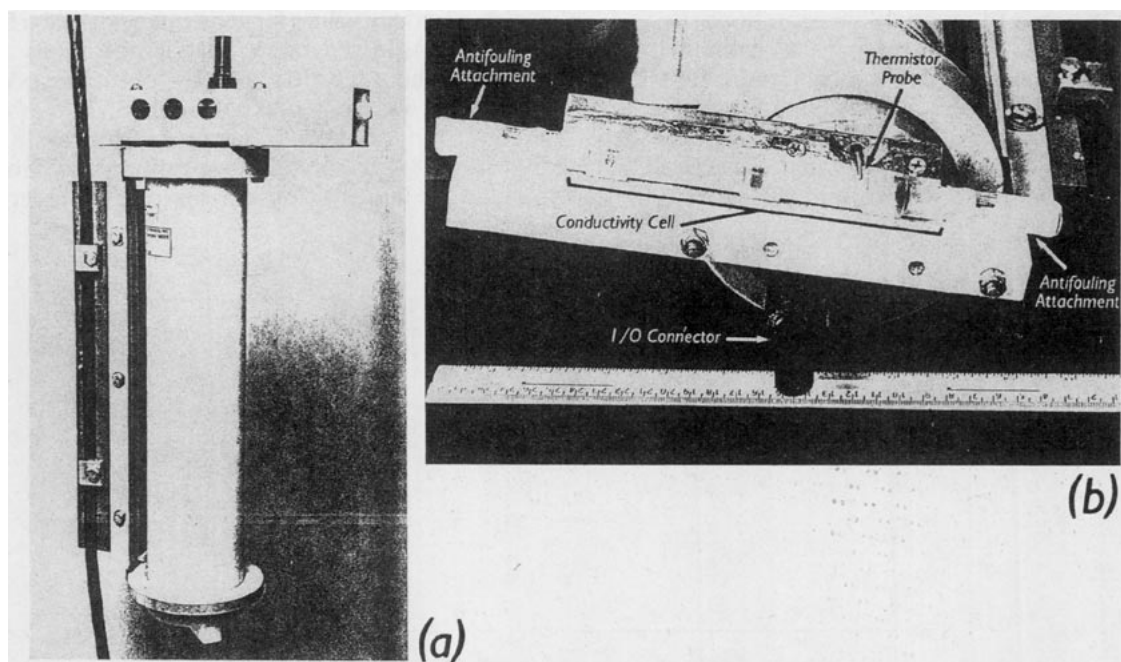


FIG. 1. (a) SeaBird model SBE-16 SEACAT mounted on a mooring line in such a way as to provide flushing of the conductivity cell by the horizontal flow field. The conductivity cell and thermistor probe are inside a protective aluminum housing atop the cylindrical plastic electronics pressure case. (b) Close-up of the conductivity cell and thermistor probe with the sensor housing removed. The grey areas inside the conductivity cell indicate locations of the three platinized electrodes.

TABLE 2. SEACAT unit numbers, dates, and depths of deployment. Maximum temperature and salinity drifts are also shown based on pre- and post-deployment calibrations for salinities in the range of 27.8 psu to 36.8 psu and for temperatures in the range of 0°C to 30°C. Maximum conductivity drifts associated with the maximum salinity drifts are indicated. Positive values indicate a spurious drift toward warmer or saltier water over the record length.

Unit	Dates	Depth (m)	$\Delta T$ (°C)	$\Delta C$ (S m <sup>-1</sup> )	$\Delta S$ (psu)
SC19	14 Oct 87–23 May 88	26	–0.002	–0.0019	–0.013
SC61	14 Oct 87–23 May 88	100	–0.002	–0.0016	–0.011
SC26	24 May 88–19 Nov 88	26	0.002	0.0009	0.006
SC27	24 May 88–19 Nov 88	100	0.002	0.0080	0.055

there was no way to determine the true orientation of the units relative to the direction of the horizontal currents. Nonetheless, we assume that flushing was adequate to produce reliable conductivity measurements since the 13-month mean scalar speeds measured by vector-averaging current meters (VACMs) at 25 m, 80 m, and 120 m were 53 cm s<sup>-1</sup>, 99 cm s<sup>-1</sup>, and 104 cm s<sup>-1</sup>, respectively. Units were set to record one sample every 30 minutes during the first deployment and every 15 minutes during the second. Table 2 shows the unit numbers, dates, and depths of deployment. The 26 m unit was placed in the weakly stratified surface layer 1 m below a VACM at 25 m; the 100 m unit was placed in the thermocline near the subsurface salinity maximum associated with the Equatorial Undercurrent (Fig. 2). Data return was approximately 95% over the duration of the experiment. The only significant data loss occurred as a result of inadequate voltage to the sensors on SC61 during April–May 1988, possibly due to the presence of mooring line vibration.

All SEACATs were pre- and post-calibrated at the Northwest Regional Calibration Center (NRCC) in Bellevue, Washington. Post-calibrations were done prior to replatinizing the conductivity electrodes so that the effects of biogenic and other material accumulating on the sensors could be determined. The absolute ac-

curacy of the NRCC calibration bath is 0.003°C in temperature and 0.003 psu in salinity. Bath resolution is 0.001°C and 0.001 psu, respectively.

Daily averaged SEACAT temperature and salinity time series data are shown in Fig. 3. Overplotted on these time series are temperatures and salinities determined from CTD casts made generally within 3 nm of the mooring. (1 nm is considered the minimum safe operating distance from the mooring for shallow CTD casts.) Casts were made with a Neil Brown Mark III CTD at the time of deployment and recovery; additional CTD casts at intermediate times were made by passing NOAA research vessels. For reference, CTD temperatures and salinities are accurate to better than 0.005°C and 0.01 psu (Mangum et al. 1980).

Figure 3 also shows the 25 m VACM temperature time series overplotted on the 26 m SEACAT time series. VACM temperatures are internally recorded as 15-minute averages, which are then block averaged to hourly and daily values for subsequent analysis (Freitag et al. 1987). In general, VACM temperatures are accurate to about 0.01°C; however, on the first deployment there was a bias of 0.05°C (SEACAT > VACM) in the first four months of the record that grew to 0.8°C by May 1988. Laboratory post-calibration of the sensors did not indicate a drift of this magnitude for either

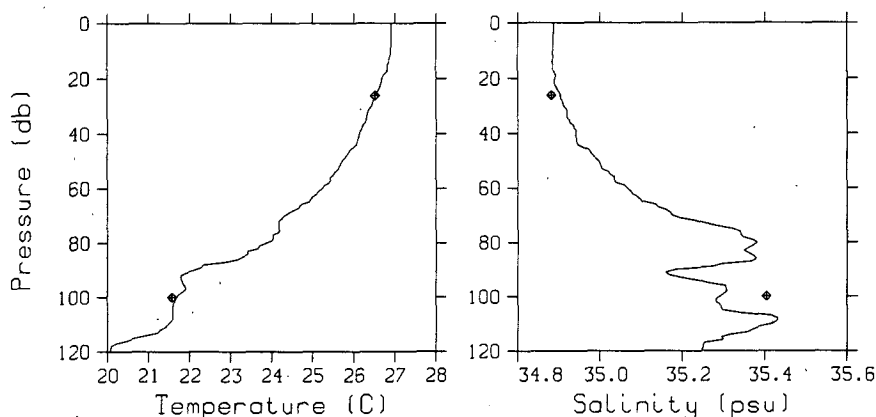


FIG. 2. SEACAT temperature and salinity measurements (◆) superimposed on a CTD profile from 0°02.1'S, 139°57.6'W on 10 November 1987. The CTD station was within 2 nm of the mooring, which was located at 0°02.6'S, 139°55.7'W.

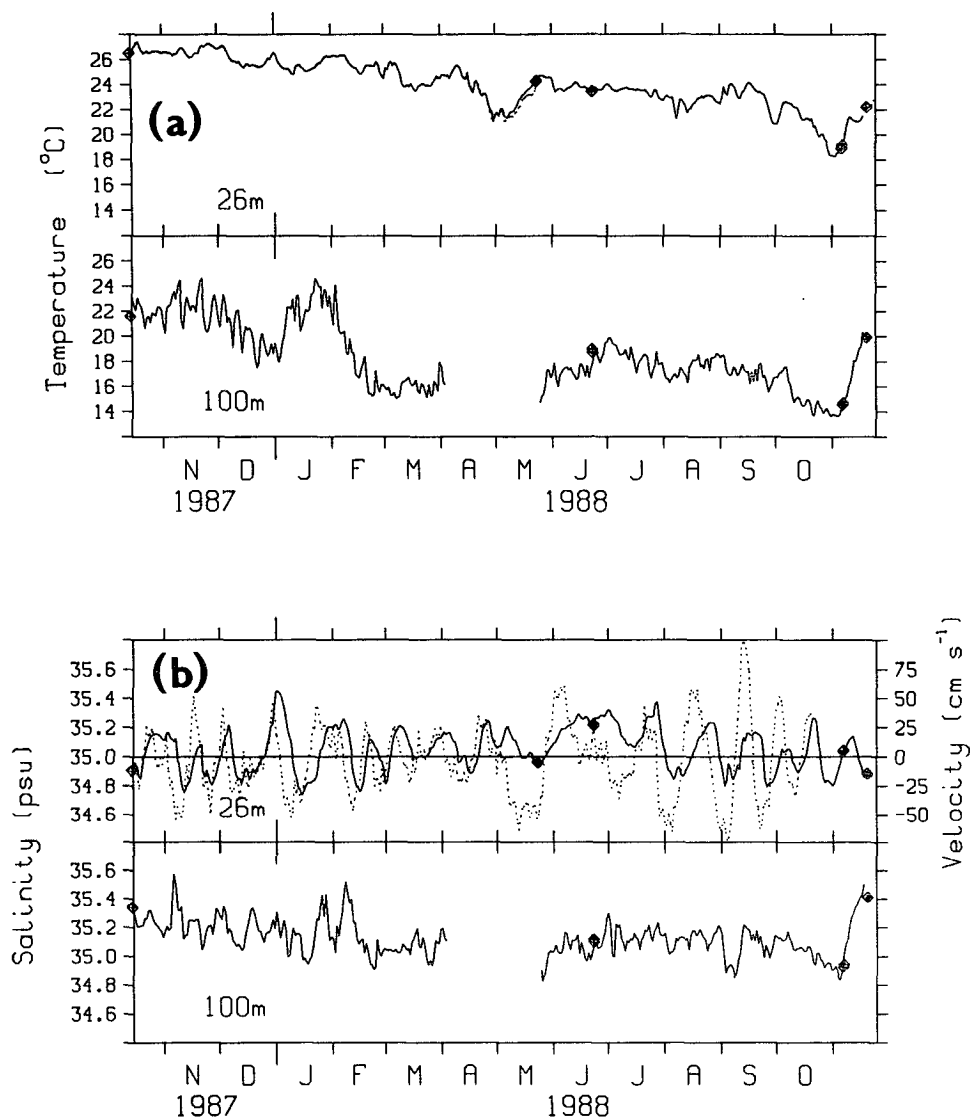


FIG. 3. Daily averaged SEACAT time series measurements of (a) temperature and (b) salinity at 26 m and 100 m. Superimposed on the 26 m temperature record is temperature from the VACM at 25 m (dashed line), which except for May 1988 is indistinguishable from the SEACAT time series (see text for discussion). Superimposed on the 26 m salinity record is meridional velocity from the 25 m VACM (dashed line). Symbols (◆) indicate temperatures and salinities determined from CTD casts typically within 3 nm of the mooring site.

instrument. While the cause of this large bias has not been determined, comparison with a temperature record at 40 m suggests that the VACM was in error.

### 3. Results

Table 2 summarizes the results of SEACAT pre- and post-deployment calibrations in terms of the maximum instrument drifts over the range of measured temperatures and salinities. In all cases, temperatures were stable to within  $0.002^{\circ}\text{C}$ . Salinities on SC19 and SC61

drifted to lower values over the first 7-month period, consistent with the expected decrease in sensitivity of the conductivity sensor due to biofouling. However, this drift was less than  $0.015$  psu. These 2 units and SC26 performed well within the manufacturer's specification of  $0.006$   $\text{S m}^{-1}$  over 6 months. On the other hand, SC27 did not perform as well due to slight leakage between the electrodes from a crack in the glass conductivity cell. This leakage resulted in a  $0.008$   $\text{S m}^{-1}$  conductivity drift and a  $0.055$  psu salinity drift between pre- and post-deployment calibrations.

TABLE 3. Summary of mean and rms differences between SEACAT and CTD measurements for October 1987–November 1988. Differences are defined as SEACAT minus CTD in degrees C and psu. Overbar denotes mean. Depths indicated are nominal depths of the SEACAT time series. See text for discussion.

Depth (m)	No. of Pairs	$\overline{\Delta T}$	$\Delta T_{rms}$	$\overline{\Delta S}$	$\Delta S_{rms}$
26	9	0.000	0.016	-0.029	0.044
100	6	-0.003	0.022	0.033	0.052

Table 3 summarizes the comparison between the CTD and SEACAT data. CTD temperature is relatively more accurate than CTD pressure; moreover, vertical motion of the surface due to gravity waves causes the SEACATs on the mooring line to heave with an amplitude of a few meters (corresponding to the significant wave height). Hence, in compiling Table 3, we chose CTD temperature/salinity (T/S) pairs, which minimized the temperature differences with the SEACATs rather than CTD measurements at the nominal SEACAT depths. In general though, these CTD T/S pairs were within a few decibars of the nominal SEACAT depths.

The differences in Table 3 are typically larger than either SEACAT or CTD instrumental errors, with the

exception of mean temperature differences. The reason is that there is a significant amount of internal wave and other small-scale variability over a few nm. Furthermore, the SEACAT sample intervals of 15 or 30 minutes often lead to several minutes' difference between the time of SEACAT measurements and the estimated time of the nearest CTD measurements. Thus, Table 3 is a pessimistic evaluation of SEACAT accuracies based on in situ comparison with CTD data. Nonetheless, differences in salinity are typically  $\sim 0.05$  psu and are ten times smaller than the range of salinities observed in Fig. 3.

Daily temperature records are plotted in Fig. 3a from the 25 m VACM and from the 26 m SEACAT. Both records show a cooling of several degrees C over the record length associated with the termination of the 1986–87 El Niño and the development of a subsequent intense, cold event (McPhaden and Hayes 1990). These temperature time series are visually indistinguishable from one another, with the exception of May 1988 when the VACM temperature sensor began to drift. The VACM thermistor was more stable during the second half of the record (May–November 1988) during which the mean VACM-SEACAT difference was  $-0.01^\circ\text{C}$  (comparable to the instrumental accuracy of the VACM). Spectra for this time period show that the SEACAT and VACM temperature measurements

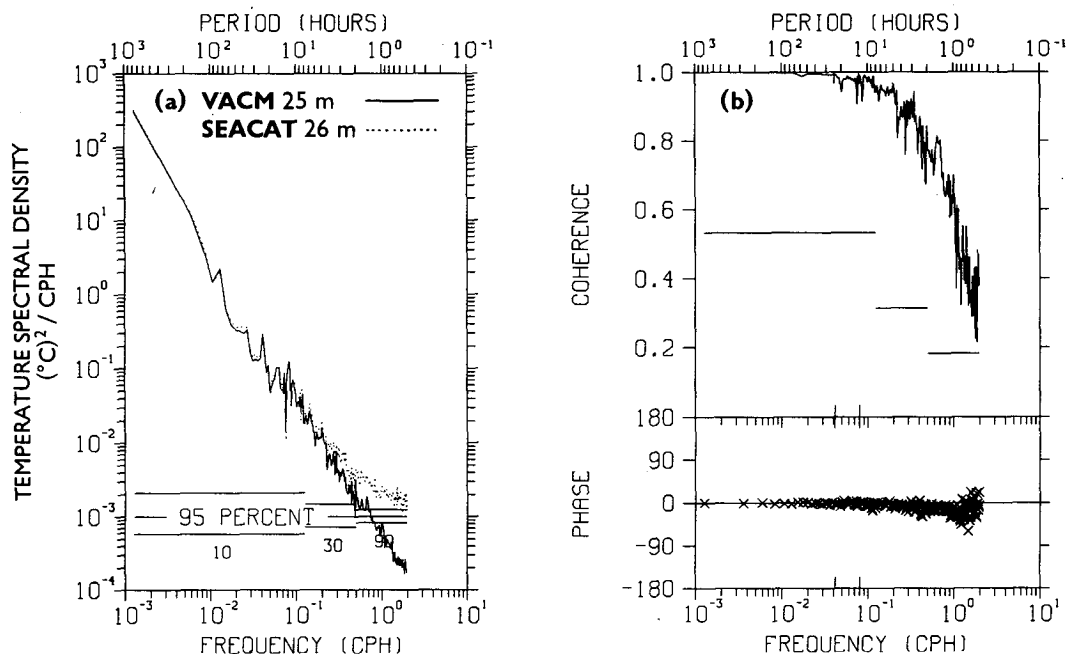


FIG. 4. (a) Autospectra of 15-minute instantaneous SEACAT temperature data at 26 m (dashed line), and 15-minute averaged VACM temperature data at 25 m (solid line) for the period 24 May to 19 November 1988. The number of frequency bands over which the spectral estimates have been computed, and the corresponding 95% confidence limits are also shown. (b) Coherence and phase spectrum for the SEACAT and VACM time series in (a). Ninety-five percent confidence limits for the null hypothesis that the two variables are statistically unrelated are shown in (b).

are indistinguishable from one another at the 95% level of confidence for all periods longer than about two hours (Fig. 4). Divergence of the autospectra, decrease in coherence and increase in phase lag at periods shorter than about four hours is due to the fact that SEACAT data are recorded as spot samples every 15 minutes whereas the VACM data are recorded as 15-minute averages. At high frequencies therefore, SEACAT data are aliased by unresolved internal waves and other short period variations that are averaged out of VACM data.

The corresponding salinity time series at 26 m (Fig. 3b) shows a dominant time scale of 20–30 days with a range of values between about 34.7 psu and 35.5 psu. These variations are strongest in boreal fall and winter and weakest in boreal spring. The 20–30 day periodicity is less pronounced at 100 m where salinities are higher on average due to proximity to the subsurface salinity maximum. A scatter diagram of SEACAT data overplotted on the mean T/S curve based on 17 EPOCS CTDs at 140°W (Fig. 5) shows these data are consistent with historical hydrographic variations.

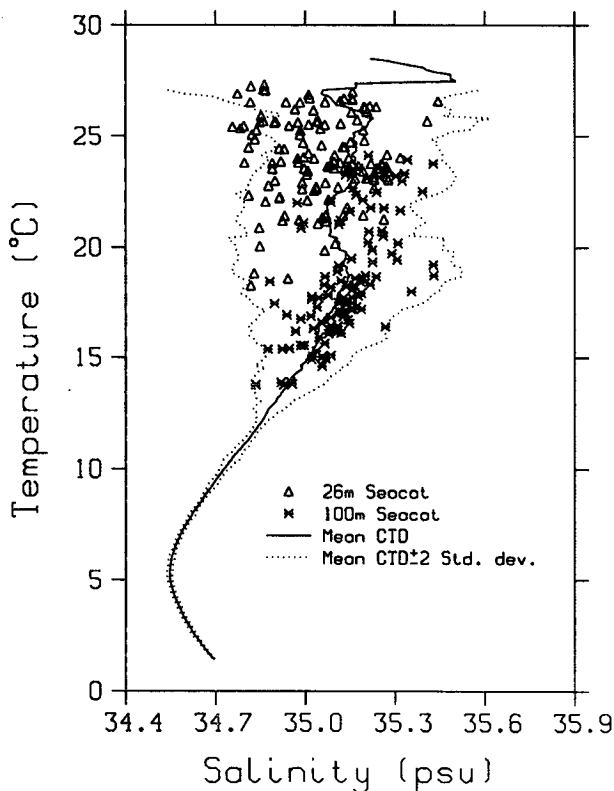


FIG. 5. Scatter diagram of SEACAT data overplotted on the mean T/S curve based on 17 EPOCS CTDs within  $\pm 0.5^\circ$  latitude and  $\pm 10^\circ$  longitude of  $0^\circ$ ,  $140^\circ$ W. Daily averaged SEACAT data are subsampled every three days. CTD data span the period 19 February 1980 to 20 November 1988. Dashed lines indicate two standard deviations as estimated from five or more CTD T/S pairs.

A physical interpretation of the observed salinity variations is that the sharp salinity front that straddles the equator (Wyrtki and Kilonsky 1984) is being advected latitudinally at the dominant time scale of the meridional velocity field. The meridional velocity at 25 m (Fig. 3c) exhibits pronounced 20–30 day fluctuations with peak-to-peak amplitudes at times of nearly  $1 \text{ m sec}^{-1}$  (see also Halpern et al. 1988). These waves are presumably generated by instability of the large-scale zonal current system (Philander 1978) and are evident in satellite infrared images as 1000 km long undulations of the sea surface temperature front in the eastern equatorial Pacific (Legeckis 1977). Figure 6 shows pronounced 30-day spectral peaks in 25 m meridional velocity and 26 m salinity, and highly significant coherence between these variables at periods between about 10–50 days. Note that the  $90^\circ$  phase difference in Fig. 6c at periods between 10 and 50 days implies that southward velocity is followed by fresher salinity and vice versa, as evident in Fig. 3b.

#### 4. Conclusion

In summary, we have examined the feasibility of making high-quality moored salinity time series measurements in the upper equatorial Pacific from 13 months of SeaBird SEACAT data near  $0^\circ$ ,  $140^\circ$ W. Laboratory pre- and post-deployment calibrations indicated that the instrumental drift in SEACAT salinity measurements was typically  $<0.015$  psu with a maximum of 0.055 psu over sequential 6–7 month long mooring deployments. The maximum drift (0.055 psu) was due to a cracked conductivity cell, which the manufacturer informs us is a problem that other users have experienced. SeaBird subsequently repaired our unit at no cost and claims that production procedures have been improved to eliminate this problem in newer units (Nordeen Larson, personal communication).

Comparison of SEACAT data with data from CTD casts made within a few nautical miles of the mooring indicate rms differences of  $\sim 0.05$  psu. Comparisons with CTD data are a pessimistic indicator of SEACAT performance because spatial and temporal variations affect the rms differences as much as instrumental errors. Nonetheless, these differences were 10 times smaller than the most energetic salinity fluctuations observed in our records.

Little biogenic material was found on the conductivity cells on recovery, though biological productivity was probably not significantly lower than usual during October 1987–November 1988. Indeed, the thermocline was shallower and sea surface temperatures were cooler than normal at  $0^\circ$ ,  $140^\circ$ W during much of 1988 (McPhaden and Hayes 1990) and there is evidence of enhanced biological uptake of nutrients in the surface layer during this time (Bender and McPhaden 1990). We, therefore, surmise that the SEACAT antifouling

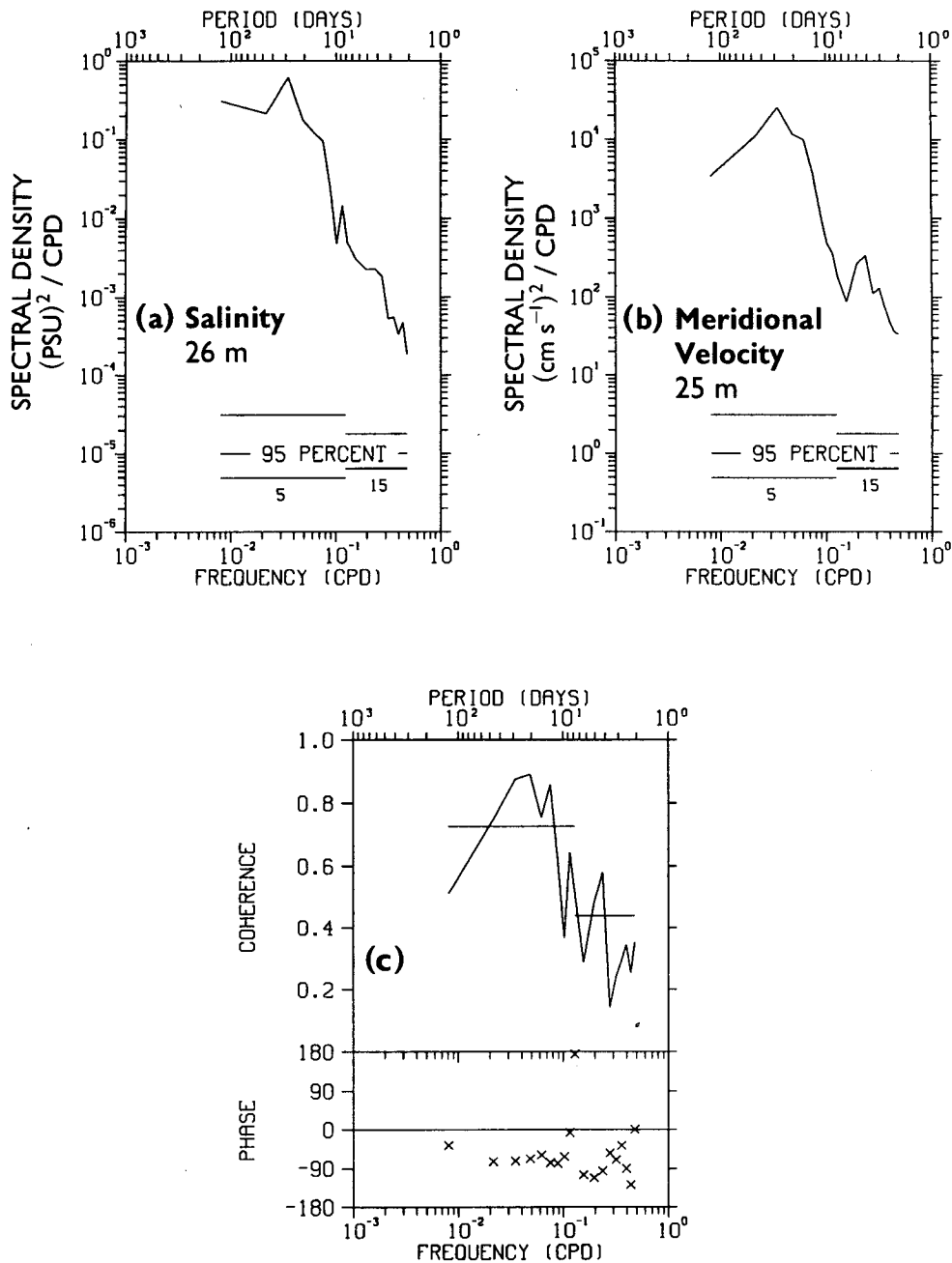


FIG. 6. Autospectra of daily averaged (a) SEACAT salinity at 26 m and (b) VACM meridional velocity at 25 m for the period 15 October 1987 to 20 October 1988. Coherence and phase between the SEACAT and VACM time series are shown in (c). Ninety-five percent confidence limits are also indicated.

compounds worked effectively and that the favorable results we obtained may be expected at different times and locations in regions of equatorial upwelling.

*Acknowledgment.* This work was supported by NOAA's Equatorial Pacific Ocean Climate Studies (EPOCS) program. Special thanks to Stan Hayes of

PMEL and Nordeen Larson of SeaBird Electronics, Inc. for comments on an earlier version of this paper.

#### REFERENCES

- Bender, M. L., and M. J. McPhaden, 1990: Anomalous nutrient distribution in the equatorial Pacific in April, 1988: Evidence for rapid biological uptake. *Deep-Sea Res.*, in press.

- Brown, W. S., J. D. Irish and C. D. Winant, 1987: A description of subtidal pressure field observations on the northern California continental shelf during the Coastal Ocean Dynamics Experiment. *J. Geophys. Res.*, **92**, 1605–1635.
- Cooper, N. S., 1988: The effect of salinity on tropical ocean models. *J. Phys. Oceanogr.*, **18**, 697–707.
- Donguy, J.-R., and A. Dessier, 1983: El Niño-like events observed in the tropical Pacific. *Mon. Wea. Rev.*, **111**, 2136–2139.
- Emery, W. J., and J. S. Dewar, 1982: Mean temperature-salinity, salinity-depth and temperature-depth curves for the North Atlantic and North Pacific. *Prog. Oceanogr.*, **11**, 219–305.
- Eriksen, C. E., 1985: The Tropic Heat Program: An Overview. *Eos, Trans. Am. Geophys. Union*, **66**, 50.
- , 1987: Observations of the seasonal cycle of upper ocean structure and the roles of advection and diapycnal mixing. *J. Geophys. Res.*, **92**, 5354–5368.
- Fofonoff, N. P., and R. C. Millard, Jr., 1983: Algorithms for computation of fundamental properties of seawater. UNESCO Tech. Pap. Mar. Sci., No. 44, UNESCO, Paris, 53 pp.
- Freitag, H. P., M. J. McPhaden and A. J. Shepherd, 1987: Equatorial current and temperature data: 108°W to 110°W; October 1979 to November 1983. NOAA Data Rep. ERL PMEL-17 (PB87-204004), 99 pp.
- Kessler, W. S., and B. A. Taft, 1987: Dynamic heights and zonal transports in the central tropical Pacific during 1979–84. *J. Phys. Oceanogr.*, **17**, 97–122.
- Halpern, D., R. A. Knox and D. S. Luther, 1988: Observations of 20-day period meridional current oscillations in the upper ocean along the Pacific equator. *J. Phys. Oceanogr.*, **18**, 1514–1534.
- Legeckis, R., 1977: Long waves in the eastern equatorial Pacific Ocean: A view from a geostationary satellite. *Science*, **197**, 1179–1181.
- Lukas, R., and E. Lindstrom, 1987: The mixed layer of the western equatorial Pacific Ocean. *Proc. 'Oha Huliko's Hawaiian Winter Workshop on the Dynamics of the Ocean Surface Mixed Layer*, University of Hawaii, Honolulu.
- Mangum, L. J., N. N. Soreide, B. D. Davies, B. D. Spell and S. P. Hayes, 1980: CTD/O<sub>2</sub> measurements during the Equatorial Pacific Ocean Climate Studies (EPOCS) in 1979. NOAA Data Rep., ERL PMEL-1 (PB81-211203), 645 pp.
- McPhaden, M. J., and S. P. Hayes, 1990: Variability in the eastern equatorial Pacific during 1986–1988. *J. Geophys. Res.*, in press.
- National Academy of Science, 1988: Report of a Drafting Workshop, AOML, Miami, on Elements of the Ten-Year Monitoring Component for El Niño and the Southern Oscillation (ENSO). Tech. Rep. USTOGA-1, University Corporation for Atmospheric Research, Boulder, 42 pp.
- Pederson, A. M., and M. C. Gregg, 1979: Development of a small in situ conductivity instrument. *IEEE J. Oceanic Eng.*, **OE-4**, 69–75.
- Philander, S. G. H., 1978: Instabilities of zonal equatorial currents, 2. *J. Geophys. Res.*, **83**, 3679–3782.
- Wyrтки, K., and B. Kilonsky, 1984: Mean water mass and current structure during the Hawaii-to-Tahiti Shuttle Experiment. *J. Phys. Oceanogr.*, **14**, 242–254.